american physiological society
JOURNAL OF APPLIED PHYSIOLOGY

J Appl Physiol 133: 517–523, 2022.
First published July 14, 2022; doi:10.1152/japplphysiol.00121.2022

RESEARCH ARTICLE

Extended lifetimes of bubbles at hyperbaric pressure may contribute to inner ear decompression sickness during saturation diving

David J. Doolette and Simon J. Mitchell

Department of Anaesthesiology, The University of Auckland, Auckland, New Zealand

Abstract

Inner ear decompression sickness (IEDCS) may occur after upward or downward excursions in saturation diving. Previous studies in nonsaturation diving strongly suggest that IEDCS is caused by arterialization of small venous bubbles across intracardiac or intrapulmonary right-to-left shunts and bubble growth through inward diffusion of supersaturated gas when they arrive in the inner ear. The present study used published saturation diving data and models of inner ear inert gas kinetics and bubble dynamics in arterial conditions to assess whether IEDCS after saturation excursions could also be explained by arterialization of venous bubbles and whether such bubbles might survive longer and be more likely to reach the inner ear under deep saturation diving conditions. Previous data show that saturation excursions produce venous bubbles. Modeling shows that gas supersaturation in the inner ear persists longer than in the brain after such excursions, explaining why the inner ear would be more vulnerable to injury by arriving bubbles. Estimated survival of arterialized bubbles is significantly prolonged at high ambient pressure such that bubbles large enough to be filtered by pulmonary capillaries but able to cross right-to-left shunts are more likely to survive transit to the inner ear than at the surface. IEDCS after saturation excursions is plausibly caused by arterialization of venous bubbles whose prolonged arterial survival at deep depths suggests that larger bubbles in greater numbers reach the inner ear.

NEW & NOTEWORTHY Inner ear decompression sickness that occurs during deep saturation diving is explained by arterialization of venous bubbles across intracardiac or intrapulmonary right-to-left shunts and growth of these bubbles if they arrive in the inner ear. Bubbles in arterial blood have prolonged lifetimes at hyperbaric pressures compared with at sea level. This can explain why inner ear decompression sickness is more characteristic of rapid decompressions at great depths than of decompression at sea level.

bubble dynamics; high ambient pressure; intrapulmonary arteriovenous anastomosis

INTRODUCTION

Inner ear decompression sickness (IEDCS) most commonly causes vestibular symptoms (vertigo, nausea, ataxia) and, less commonly, cochlear symptoms (tinnitus, hearing loss) (1). In ~75% of cases, inner ear symptoms are the only manifestation of decompression sickness (DCS) (2). Previously, IEDCS seemed to be associated with deep dives using heliox or trimix, but it has been increasingly seen after air dives, albeit at the deeper end of the recreational range (1, 2). IEDCS symptoms may arise after surfacing, typically with short latency (within 30 min) (2). This is the most common pattern after recreational air dives and is also seen after deep heliox or trimix dives. IEDCS may also arise before surfacing during decompression from deep dives and during subsurface ascents in saturation diving. In deep dives, onset has occasionally been temporally associated with breathing gas switches from helium-rich mixes to air or nitrox mixes (3).

Multiple pathophysiological paradigms for IEDCS have been proposed. One possibility is the formation of "autochthonous" bubbles from supersaturated gas within the inner ear itself. This supersaturation may result from decompression or from inert gas counter-diffusion after switches from helium-rich to nitrogen-rich breathing mixtures (3). Also, the strong association between inner ear DCS and the presence of a right-to-left shunt (RLS), such as a large persistent (patent) foramen ovale (PFO), reported in multiple studies cited in the article by Mitchell and Doolette (2), suggests that venous gas bubbles (also called venous gas emboli or VGE) crossing an RLS can be causative (2, 4). In the latter paradigm, arterialized VGE are more likely to cause injury if they reach a tissue that is gas supersaturated where inward diffusion of gas causes them to grow. Slower inert gas elimination and more prolonged supersaturation in the inner ear than in the brain provide an explanation for the selective vulnerability of the inner ear compared with the brain when both are exposed to arterialized VGE (5).

In this article, we explore the hypothesis that IEDCS occurring after excursions in saturation diving is also a result of VGE crossing an RLS and reaching the inner ear while it remains supersaturated, allowing these tiny bubbles to grow and cause injury. We first review existing evidence that

Correspondence: D. J. Doolette (david.doolette@auckland.ac.nz).
Submitted 28 February 2022 / Revised 5 July 2022 / Accepted 8 July 2022

IEDCS is characteristic of excursion decompression in saturation diving and that these decompressions are associated with VGE formation. We then use our previously published gas kinetic models to investigate whether these decompressions also produce substantial inner ear gas supersaturation. Finally, we use models of bubble dynamics to explore the possibility that bubbles could have prolonged lifetimes in pulmonary venous and systemic arterial blood at greater depths, which would increase the likelihood that VGE can survive long enough to become arterialized (via a PFO or transpulmonary passage) and reach the inner ear.

SATURATION EXCURSIONS, IEDCS, AND VGE

Saturation diving is a technique for diving where divers live for days or weeks in a dry chamber at a "storage depth" and periodically enter the water to perform work. Divers undergo very slow "saturation decompression" (typically $\leq$12 kPa·h^{-1}) to the surface at the end of the operation. Commonly, divers make descents (downward excursions) to complete underwater tasks and then return to storage depth. Divers may also ascend above storage depth (upward excursion) to complete underwater tasks and then return to storage depth. Less commonly, upward excursions are made in the dry chamber to change storage depth or commence saturation decompression. Decompression during these excursions can be as fast as 184 kPa·min^{-1}, much faster than saturation decompression. DCS occurring during saturation decompression usually manifests as musculoskeletal pain (6, 7). In contrast, DCS arising from an upward excursion from storage depth or following a long-duration downward excursion is often severe, occasionally with spinal manifestations, but more commonly is IEDCS without other manifestations arising during or shortly after decompression. Published cases of IEDCS from saturation-excursion diving are mostly from experimental dives with upward or downward excursions of greater magnitude than that used in current operational diving.

The U.S. Navy unlimited duration excursion limits were published in 1978 and subsequently revised twice (8). These limits are the maximum distance upward excursion that can be made at 184 kPa·min^{-1} from saturation at a particular storage depth to a shallower storage depth, but these excursion distances are also used to make downward excursions with no restriction on bottom time and direct decompression back to storage depth. There are two published reports describing eight DCS cases (Table 1) attributable to upward excursions using the earlier U.S. Navy limits (8, 9). There were two cases of musculoskeletal DCS, one case of serious spinal DCS, and five cases of IEDCS; all but one IEDCS occurred within an hour after the decompression (8, 9). The upward excursions that resulted in serious manifestations were greater than the current limits. IEDCS after excursions also occurred during the development of saturation diving procedures at the Royal Navy Physiological Laboratory, although musculoskeletal DCS was equally common (Table 1). IEDCS resulted from upward excursions from 791 to 571 kPa and during rapid initial decompression ($\geq$ 110 kPa·h^{-1}) from a very deep (4.7 MPa) saturation dive (10, 11).

IEDCS also occurs after decompression from long-duration downward excursions (Table 1). During "Predictive Studies IV" saturation dives conducted at the University of Pennsylvania, a total of 25 excursions were made from 2.71 MPa storage to 3.78 MPa or from 3.78 MPa storage to 5.00 MPa. Excursions were of various durations, and the 11 longest excursions (20–40 min of compression and 55 min at the bottom) resulted in two IEDCS and one spinal DCS either during or shortly after decompression back to storage depth (13). During the Janus IV saturation dive conducted at the

Table 1. *DCS after saturation excusions*

No. of Excursions	No. of IEDCS	No. of Spinal DCS	No. of Pain-Only DCS	P1*, MPa	P2†, MPa	% USN Upward‡	Deco. Rate, kPa·min^{-1}	VGE§, No/Yes/HG	Reference
Upwards									
104	5	0	1	4.39	3.67	131%	184	0/5/1	(8)
				2.06	1.69	103%	184		
245	0	1	1	3.17	2.5	133%	184		(9)
12	2	0	4	0.79	0.57	105%	120		(10)
2	1	0	0	4.70	4.02	119%	2		(11)
12	0	0	3	3.10	2.60	111%	100	1/11/8	(12)
Downwards									
25	2	1	0	5.00	3.78	209%	14	0/11/NA	(13)
				3.78	2.71	213%	10		
39	1	0	0	4.70	4.10	105%	10	31/8/2	(7)
Bounce									
68	1	0	0	2.20	1.13	382%	5	51/17/5	(7)
15	3	1	0	2.09	1.48	168%	7		(14)
				2.09	1.54	151%	28		
315	11	NA	NA	3.10	1.7	311%	4		(15)
				1.60	0.58	329%	8		

*Ambient pressure from which excursion decompression was initiated; for multiple P1, the deepest and shallowest resulting in severe DCS are given. †Ambient pressure of symptom onset or end of excursion, the latter being either a hold at storage depth or transition to saturation decompression rates ($\leq$12 kPa·h^{-1}); if more than one excursion resulted in IEDCS, the largest excursion (lowest P2) is given. ‡% of current U.S. Navy upward excursion limit for dives resulting in severe DCS. P1, P2, excursion distances, and decompression rates are for excursions resulting in DCS but are representative of all excursions in series. §No: number of excursions for which no VGE were detected/Yes: number of excursions for which any VGE were detected/HG: number of excursions for which high-grade VGE were detected. IEDCS, inner ear decompression sickness; DCS, decompression sickness; NA, not available; VGE, venous gas emboli.

commercial diving company Comex, a downward excursion from 4.10 MPa storage depth to 4.70 mPa for 4.5 h resulted in IEDCS 30 min after return to storage (7). Comex also reported three IEDCS cases resulting from downward excursions from 1.30 MPa storage depth to 1.90 MPa, but no other details of these cases are available, and they do not appear in Table 1.

IEDCS has also been described during decompression from extremely deep and long-duration heliox bounce dives (nonsaturation dives of hours rather than days in duration) that resemble saturation-excursions (7, 14, 15). These "excursion-like" bounce dives were to depths (1.6–3.1 MPa) more typical of saturation dives and for long bottom times (1–6 h). Although the latter stages of decompression from these bounce dives approach saturation decompression rates, IEDCS occurred during the rapid initial decompression from maximum depth (Table 1).

VGE measurements using precordial Doppler have been made following excursions in five of the series summarized in Table 1 and one other saturation dive not included in Table 1 because of insufficient details in the only available report. Bubble profusion was usually reported with the Spencer scale of five ordinal grades from 0 (no bubbles) to IV (continuous bubble signals overriding cardiac sounds) (16). High-grade VGE were defined as ≥grade II (bubble signals in many but less than half of cardiac cycles) at rest or ≥grade III (bubble signals in most cardiac cycles but not overriding cardiac sounds) with movement. The dive not included in Table 1 was a 152-msw (1.62 MPa) saturation dive conducted at the Defence and Civil Institute of Environmental Medicine during which five divers made several upward excursions to 121 msw (1.31 MPa, current U.S. Navy limit), and high-grade VGE (grade II–III at rest) were detected in two divers (17).

Of the excursions summarized in the first two rows of Table 1, VGE measurements have only been reported for Navy Experimental Diving Unit (NEDU) Deep Dive 81. A single VGE measurement was made in each diver immediately following an upward excursion from 3.17 MPa to 2.66 MPa (110% of the current U.S. Navy limit). VGE were not detected in the first diver insonated but were detected in the other five divers, with a high grade (grade III at rest) in one diver (8, 17). VGE measurements were made during and following decompression from 11 of the 12 Predictive Studies IV downward excursions from 3.78 MPa to 5.00 MPa (row 7 of Table 1). VGE were not conventionally graded but were detected throughout decompression and after reaching storage depth in all 11 excursions (13). During the Norwegian Underwater Institute DEEP-EX 80 saturation dive, two upward excursions were made from 3.10 MPa to 2.60 MPa (row 6 of Table 1), and VGE were detected in all six divers and following both excursions in five of the divers. An unconventional, Spencer-like grading system was used by which eight excursions resulted in grades II to IV VGE at rest. Notably, bubbles were also detected in the carotid and other arteries in all divers, with grades II to III at rest in three of the divers (12).

In dive series with incidents of IEDCS and VGE detection, there is a general association of IEDCS with excursions with high VGE grades. During NEDU Deep Dive 81, IEDCS occurred 35 min after the upward excursion in the only diver with high-grade VGE (8, 17). During the Comex Janus IV saturation dive, the one incident of IEDCS followed one of the two excursions that resulted in high-grade VGE (7). Similarly, the incident of IEDCS during decompression from the Comex excursion-like bounce dives occurred in one of the five dives that resulted in high-grade VGE (7). The Predictive Studies IV saturation dive provides something of an exception. Each of the four divers made three downward excursions from 3.78 Pa to 5.00 MPa, and one excursion resulted in IEDCS 18 min after reaching storage depth. However, the diver with IEDCS was a "low-bubbler," consistently having the lowest bubble count per minute in the pulmonary artery of all four divers (13). Contrary to the association of IEDCS with high-grade VGE following excursions, IEDCS is never reported during saturation decompression, although high-grade VGE commonly occur (7, 13, 17).

METHODS

Our physiological model of inner ear gas kinetics has parameters based on the published literature, the structure and validation of which have been detailed previously (3). Three well-stirred compartments represent the membranous labyrinth (the vascular compartment), the perilymph, and the endolymph. Inner ear gas uptake and washout occur via perfusion equilibration of the membranous labyrinth with arterial blood and, negligibly, by diffusion across the round window. Within the inner ear, gas diffuses between the membranous labyrinth and each of the labyrinthine fluid compartments across diffusion-limited membranes of zero volume. The diffusion time constants across these membranes were formulated to reflect the geometry of the inner ear. Such compartmental diffusion models provide a first-order approximation of diffusion kinetics.

A well-established model of cerebral inert gas kinetics was used to represent the brain. This model was constructed by estimating the volume of a single, well-stirred compartment by fit of the model to the arterial and sagittal sinus nitrogen and helium concentrations and sagittal sinus blood flows measured during sequential breathing of different inert gases and changes in cerebral blood flow in anesthetized sheep (18). For the present simulations, a normal cerebral blood flow of 55 mL·100 g^{-1}·min^{-1} was assumed.

To simulate the dissolution of a spherical bubble in pulmonary venous and systemic arterial blood, we use a three-region, well-stirred tissue ("3RWT") model in which the three regions are the bubble, a shell of liquid surrounding the bubble across which gas diffuses, and a region outside the shell with uniform gas partial pressure (well stirred) (19, 20). The 3RWT model is physiologically plausible because the flowing blood is assumed to be well stirred so that diffusion occurs only through a thin layer near the bubble surface. The development of the 3RWT model is detailed in Ref. 19 and Ref. 20, and only key features are described here.

We model the survival of arterialized VGE at constant depth and steady-state arterial conditions, as would prevail from several minutes after decompression when VGE are typically first detected and when IEDCS typically onsets. We assumed that oxygen, carbon dioxide, and water vapor are in equilibrium between the bubble and surrounding blood, and for simplicity, we do not model the change from venous to arterial values. As a result, the sum of oxygen, carbon

dioxide, and water vapor partial pressures is a fixed contribution to bubble pressure (P_{fix}). The change in bubble size is then the result of diffusion of one inert gas (i), e.g., helium or nitrogen.

The pressure of inert gas i in a spherical bubble not in contact with a surface or subject to any tissue elastic forces is given by:

$$P_i = P_{amb} + \frac{2\gamma}{r} - P_{fix} \quad (1)$$

where P_{amb} is the ambient pressure, γ is the surface tension of the liquid, and r is the bubble radius at the gas/liquid interface.

The flux of inert gas i across the bubble surface is given by Fick's first law:

$$\frac{d(P_i V_{bub})}{dt} = AD_i\alpha_i g_i \quad (2)$$

where V_{bub} is the volume of the bubble ($V_{bub} = 4\pi r^3/3$), A is the surface area of the bubble, D is the diffusion coefficient of gas i in the liquid, $\alpha = H^{cp}RT$ is the liquid-gas partition coefficient in the liquid (H^{cp} is the Henry's law constant, R is the universal gas constant, and T is temperature), and g_i is the inert gas partial pressure gradient at the bubble surface. Combining *Eqs. 1* and *2* and solving for change in r results in:

$$\frac{dr}{dt} = \frac{\alpha_i D_i g_i - \frac{r}{3}\cdot\frac{dP_{amb}}{dt}}{P_{amb} - \sum P_{fix} + \frac{4\gamma}{3r}} \quad (3)$$

For the 3RWT model, the solution for the inert gas gradient g_i assumes spherical symmetry in the diffusion region and assumes the bubble equilibrates with the surrounding liquid much faster than changes in gas partial pressures in the liquid, such that the explicit time-dependent term of the diffusion equation can be ignored (quasi-static approximation):

$$g_i = \left(\frac{1}{h} + \frac{1}{r}\right)(P_{ws} - P_i) \quad (4)$$

in which h is the thickness of the shell of liquid surrounding the bubble through which gas diffuses, and P_{ws} is the inert gas partial pressure in the well-stirred region outside the shell. The 3RWT model has been used to model decompression bubbles in extravascular tissue and blood using different values for h (19–22). Here, we will use two versions. We will either set h = 1 μm or we will assume h varies with bubble radius according to $h = Z(1-e^{-r/Z})$, with Z = 50. The latter has h near Z for large bubbles and converges with bubble radius for smaller bubbles and was found to match the dissolution of large nitrogen bubbles in water (23).

We assume that the pulmonary venous blood has the same gas partial pressures as systemic arterial blood (P_{H2O} = 6.26 kPa and Pa_{CO_2} = 5.12 kPa). For air breathing at the surface, Pa_{O_2} = 14.92 kPa, and for a PI_{O_2} of 40.5 kPa common in saturation diving, Pa_{O_2} = 35.43. $P_{a,INERT} = P_{ws} = P_{amb} - P_{fix}$. Blood surface tension is 56 dyne·cm^{-1} = 56 kPa·μm (24). D_{He} = 9,300 μm^2·s^{-1}, α_{He} = 0.0094, D_{N2} = 2,900 μm^2·s^{-1}, and α_{N2} = 0.0151 (25).

Bubble dynamics were simulated numerically by iterative solution of *Eq. 1* and *Eq. 3* (the latter incorporating *Eq. 4*) using the LSODA variable step size differential equation solver in the deSolve package of R (v. 4.0.5. R Core Team. R: A language and environment for statistical computing. Vienna: R Foundation for Statistical Computing, 2021. URL: https://www.R-project.org/). The R scripts are freely available at https://github.com/Doolette/SatArtBubIE.

RESULTS

Figure 1 shows the calculated gas partial pressures in the brain and the inner ear for the upward excursion in NEDU deep dive 81. For clarity, only the inner ear compartment representing the membranous labyrinth is shown. Gas partial pressures in the compartments representing the endolymph and perilymph follow similar time courses. It is the membranous labyrinth that is vascularized, and it is this gas partial pressure to which arterial gas emboli entering the inner ear would be exposed. It is clear from Fig. 1 that supersaturation in the inner ear is initially substantial (peak 383 kPa) and is prolonged during and after the upward excursion. This period of supersaturation approximately coincides with the onset of IEDCS 35 min after this excursion. Figure 1 also shows that there is only a brief period of supersaturation in the brain. During saturation decompression (not illustrated), the inner ear is never supersaturated because the decompression rates are slow relative to inner ear gas kinetics.

Figure 2 shows the change in diameter of spherical bubbles in the pulmonary venous or systemic arterial blood. The figure shows the dynamics for a bubble in which the inert gas is nitrogen for a diver at sea level breathing air and for a bubble in which the inert gas is helium for a diver at 2.6 MPa breathing heliox (constant PIO_2 = 40.5 kPa). The latter conditions are those when venous and arterial bubbles were detected in all divers during the Norwegian Underwater Institute DEEP-EX 80 saturation dive. For both scenarios,

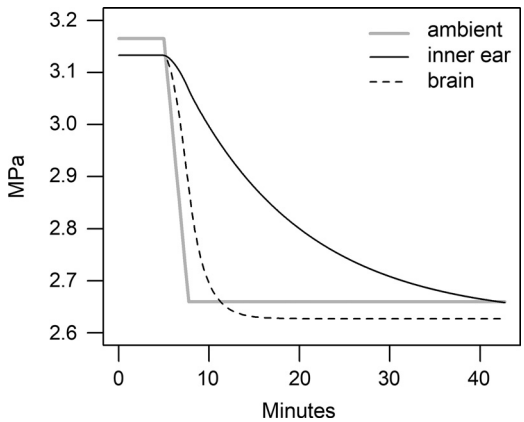

Figure 1. Simulation of inner ear and brain gas pressures during an upward excursion in NEDU Deep Dive 81 that resulted in IEDCS with onset 35 min after the excursion. The absolute ambient pressure is shown in gray. The sum of compartmental gas partial pressures for the vascularized membranous labyrinth (inner ear, solid black line) and for cerebrum (brain, dashed black line) includes a fixed contribution of 19 kPa representing oxygen, carbon dioxide, and water vapor. Note the prolonged supersaturation in the membranous labyrinth compared with the cerebrum. Arterialized VGE will not grow if they reach the tissue after the period of supersaturation. IEDCS, inner ear decompression sickness; VGE, venous gas emboli.

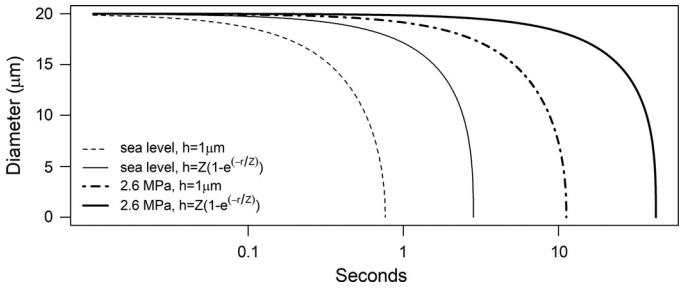

Figure 2. Simulation of dissolution of spherical bubbles with initial diameter of 20 μm in pulmonary venous blood or arterial blood. Curves are for a nitrogen-rich bubble in a diver at sea level breathing air and for a helium-rich bubble in a diver at 2.6 MPa breathing heliox. The latter conditions are those when venous and arterial bubbles were detected after an upward excursion during the Norwegian Underwater Institute DEEP-EX 80 saturation dive.

there are curves for models with the fixed and the variable diffusion region thicknesses. The figure illustrates a bubble with an initial diameter of 20 μm, which is confluent with previously measured VGE and too large to pass through pulmonary capillaries but could cross an RLS (26, 27). The 20-μm-diameter bubble persists for 0.77 to 2.8 s at sea level and for 11 to 42 s at 2.6 MPa. Bubbles of different sizes will have different lifetimes. For instance, 30-μm-diameter bubbles (not illustrated) persist for 1.7 to 9.0 s at sea level and for 26 to 140 s at 2.6 MPa, and 6.5-μm-diameter bubbles (small enough to travel through a pulmonary capillary) dissolve in 0.081 to 0.13 s at sea level and in 0.93 to 1.5 s at 2.6 MPa.

DISCUSSION

The occurrence of IEDCS after excursions but not during saturation decompression can be explained if this injury arises from arterialization of VGE that reach the inner ear microcirculation, as has been previously proposed for bounce diving. In that paradigm, arterialized VGE are much more likely to cause injury if they reach a tissue that remains gas supersaturated where bubbles will grow by inward diffusion of gas (2, 5). In tissues that are not supersaturated (such as the brain), bubbles will dissolve or pass through the capillary bed and, generally, not cause injury. Thus, the patterns of supersaturation shown in Fig. 1 explain why arterialized VGE would result in injury to the inner ear but not the brain. Similarly, that the inner ear is never supersaturated during saturation decompression can explain why IEDCS is never seen in that setting, despite high-grade VGE commonly occurring.

It is acknowledged that given the substantial and long-lasting supersaturations in the inner ear after upward excursions, the formation of autochthonous bubbles from supersaturated gas within the inner ear itself must be considered as an alternative cause for IEDCS. A study of animals subjected to bounce dives found evidence of vascular injury and assumed this to be due to local intravascular bubble formation (28). However, all tissues with half-times slower than the inner ear will have greater and more prolonged local supersaturation than the inner ear after an upward excursion. These tissues would include those likely injured by autochthonous bubble formation to produce musculoskeletal pain in DCS. Thus, if IEDCS were caused by autochthonous bubbles, one might expect it to be less common than musculoskeletal DCS (pain) after an upward excursion, whereas the opposite is reported. This latter argument admittedly takes no account of potential differences in the sensitivity of tissues to bubble formation.

The lungs are normally efficient at filtering and eliminating venous bubbles, presumably because VGE (diameter 19–700 μm) pass into a capillary bed (mean diameter 6.5 μm) (26, 27, 29). Under these circumstances, transpulmonary transit of bubbles is delayed and bubbles dissolve as gas diffuses from inside the bubbles to the alveolar gas. An RLS that allows arterialization of VGE may be intracardiac (PFO or atrial septal defect) or intrapulmonary arteriovenous anastomoses (IPAVAs). Both intracardiac shunts and IPAVA can be detected using agitated bubble contrast echocardiography and are distinguished by differences in the time for right-to-left transit. The anatomic size of IPAVA is unknown, but their detection using agitated bubble contrast, which is quoted as containing air bubbles with a mean diameter of 30 μm (30), indicates that IPAVA can conduct bubbles of sizes that would normally be removed by pulmonary capillaries. Divers without intracardiac shunt arterialize VGE produced by decompression, presumably through IPAVA, and the proportion of divers with an RLS increases from rest to ∼95% during exercise (31). Although the PFO status of the cases reported in Table 1 is unknown, all divers have the potential to arterialize VGE via IPAVAs. It is striking that in the only study that made Doppler measurements at arterial sites, arterial bubbles were detected after upward excursions in all six divers (12). This finding may be indicative of arterialization of VGE through IPAVA because it is unlikely that all six divers had PFO, since the typical prevalence of PFO in divers is 25% (2).

For VGE to reach the labyrinthine artery, they must survive long enough to traverse the pulmonary capillaries or an RLS and travel from the left heart to the posterior cerebral circulation. If the VGE pass through a PFO or other intracardiac shunt, the right-to-left transit may be virtually instantaneous (<1 s), as is frequently observed in bubble contrast echocardiography. Normal left ventricle ejection fraction is ≥ 60%, so some arterialized bubbles will swirl within the chamber (as seen during echocardiography). Nevertheless, it seems reasonable to assume that some bubbles transit from the left atrium, through the mitral valve and the left ventricle in a single cardiac cycle, e.g., within 1 s. In the case of IPAVA, this transit will take longer. In saline contrast echocardiography, a delay of at least three cardiac cycles between bubble opacification of the right heart and the appearance of bubbles in the left heart is cited as indicative of IPAVA transit (31). In terms of timing, this will amount to several seconds, and published exemplars include a 5-s delay (32). Whether the entirety of this transit should be considered an exposure to arterial conditions is doubtful, given these anastomoses must join the pulmonary veins distally. Since the gaseous milieu within anastomotic blood cannot be known with certainty, it seems reasonable to attribute half the transit to arterial conditions (e.g., 2.5 s). If VGE must pass through the pulmonary capillaries, the cardiopulmonary transit time from right to left ventricle in resting subjects is ∼6.5 s, of which >80% (i.e., ∼5 s) is after the pulmonary arterial pathway (33).

Arterial transit of small bubbles from the left heart to the cerebral circulation is likely rapid but modeling this process is

challenging. One attempt estimated a 1-s transit but ignored transit through the labyrinthine artery itself, focused on the wrong large proximal conduits (carotids rather than the vertebrobasilar system), and incorrectly assumed each artery receives the full cardiac output (22). Similar calculations using published lengths, internal diameters, and blood flows for the aorta, aortic arch or brachiocephalic artery, and subclavian and vertebral arteries result in arterial transit times from the left heart to the distal end of the left and right vertebral arteries of 1.3 and 1.6 s, respectively (34, 35). To these values, we add 200 ms transit time between the vertebral and the basilar artery, as indicated by arterial spin labeling angiography (36), and round up to 2 s to accommodate labyrinthine artery transit, to approximate arterial transit time from the left heart to the inner ear.

An approximate distillation of the previous paragraph would suggest that in transit to the inner ear, VGE will be exposed to arterial conditions for at least 3 s if they cross a PFO, 5.5 s if they cross an IPAVA, and 8 s if they transit the pulmonary capillary bed. During this transit, bubbles will shrink, as inert gas diffuses down its concentration gradient from inside to outside the bubble. At hyperbaric pressures, the gas inside a bubble is denser, and the flux of gas out of the bubble results in a smaller volume change than at sea level. Consequently, bubbles of the same diameter will shrink more slowly and have longer lifetimes at hyperbaric pressures than at sea level. The present estimated lifetimes of VGE small enough to readily transit the pulmonary capillary bed suggest that they are unlikely to survive transit to the inner ear by any route, whether at the surface or during deep diving. This suggests that arterialization via a PFO or IPAVA is the more relevant mechanism for IEDCS in saturation diving. Figure 2 is an example of a VGE (20 μm diameter) too large to pass through the pulmonary capillaries, that is unlikely to survive the transit through a PFO or IPAVA to the inner ear at sea level but can survive these same transits at 2.6 MPa. VGE that can survive transit through a PFO or IPAVA to the inner ear both at sea level and at hyperbaric pressure would reach the inner ear at a larger size at hyperbaric pressure. The larger number and the sizes of bubbles that can reach the inner ear (irrespective of the route of arterialization) at hyperbaric pressure potentially influence the consequent risk of IEDCS. This may explain why IEDCS is the most reported manifestation of DCS after excursions at great depths.

The extent to which hyperbaric pressure in saturation diving increases the number and the sizes of bubbles that can reach the inner ear depends on the actual bubble dynamics, of which we cannot be certain. We recognize that there are conceptual difficulties with the 3RWT model, particularly that equal gas flux at the inner and outer boundaries of the shell results in constant shell gas content despite changing shell volume (20). Even accepting the 3RWT approximation, the thickness of the diffusion layer (h) has a large effect on bubble lifetime, and there are no relevant experimental data of spherical bubble dynamics in blood with which to validate any model. Nevertheless, we believe our two formulations of h are physiologically plausible. A constant thickness shell h = 1 μm could represent a shell of proteins or other blood constituents accreted to a bubble, and simulations with h = 1 μm represent the shortest likely bubble lifetimes. The simulations with this formulation indicate an important increase of bubble lifetimes at ambient pressure characteristic of saturation diving. A shell with thickness varying with bubble radius according to $h = Z(1-e^{-r/Z})$ could represent a layer of stagnant blood surrounding the bubble. We acknowledge that larger values of h and longer bubble lifetimes are possible.

The current U.S. Navy unlimited duration excursion limits are the result of revisions in response to incidents of IEDCS with the older limits (8), and DCS experience specifically with the current limits has not been published. Many commercial diving companies have developed even more conservative saturation-excursion procedures that allow only a fraction of the excursion distance of the U.S. Navy excursion limits, require a long hold at storage depth after a downward excursion before commencing saturation decompression, and prohibit upward excursions to initiate saturation decompression (37). Analysis of such reduced limits indicates that they should result in less VGE than the U.S. Navy limits (37). The present results support saturation-excursion procedures that limit VGE during the first hour after decompression. The use of conservative saturation-excursion procedures is also supported by the experience of their use in the Norwegian petroleum production industry, which has reported no decompression sickness of any type between 2003 and 2021 despite ~10,000 to 140,000 annual man-hours of saturation diving (38).

This low incidence of IEDCS in modern saturation diving makes standard approaches to investigating causal relationships extremely difficult. For instance, it would be useful to investigate the association of PFO with IEDCS in saturation diving because it may be less strong than is the case for bounce diving. After bounce diving, rapid transit of VGE to the left heart via a PFO is important because of the relatively short lifetimes of bubbles at sea level; however, alternate routes of arterialization of VGE may become increasingly relevant when bubble lifetimes are prolonged at hyperbaric pressures. Unfortunately, ever acquiring a sample of saturation divers with IEDCS large enough for statistical evaluation is unlikely. We acknowledge the limitations of our modeling approach but nevertheless believe that it provides a plausible argument for our hypothesis.

Conclusions

The strong association between IEDCS and right-to-left shunts in bounce diving reported by multiple studies constitutes a powerful argument that arterialized VGE arriving in the inner ear circulation are involved. This paper demonstrates the likely role of arterialized VGE in IEDCS following saturation excursions by showing, first, historic data demonstrating that such excursions result in VGE formation; second, that in saturation conditions, bubbles can persist in the arterial circulation longer than would be the case at surface pressure, and therefore, VGE are more likely to reach the inner ear in greater numbers and larger sizes; and third, that the inner ear remains significantly supersaturated during and following such excursions so that arriving bubbles will grow. We conclude that, as in bounce diving, IEDCS following saturation excursions is most likely caused by arterialization of VGE early after the decompression, with the growth of bubbles facilitated by inward diffusion of supersaturated gas from the surrounding inner ear tissue.

DISCLOSURES

No conflicts of interest, financial or otherwise, are declared by the authors.

AUTHOR CONTRIBUTIONS

D.J.D. conceived and designed research; D.J.D. performed experiments; D.J.D. analyzed data; D.J.D. and S.J.M. interpreted results of experiments; D.J.D. prepared figures; D.J.D. and S.J.M. drafted manuscript; D.J.D. and S.J.M. edited and revised manuscript; D.J.D. and S.J.M. approved final version of manuscript.

REFERENCES

1. **Lindfors OH**, **Raisanen-Sokolowski AK**, **Hirvonen TP**, **Sinkkonen ST.** Inner ear barotrauma and inner ear decompression sickness: a systematic review on differential diagnostics. *Diving Hyperb Med* 51: 328–337, 2021. doi:10.28920/dhm51.4.328-337.
2. **Mitchell SJ**, **Doolette DJ.** Pathophysiology of inner ear decompression sickness: potential role of the persistent foramen ovale. *Diving Hyperb Med* 45: 105–110, 2015.
3. **Doolette DJ**, **Mitchell SJ.** Biophysical basis for inner ear decompression sickness. *J Appl Physiol (1985)* 94: 2145–2150, 2003. doi:10.1152/japplphysiol.01090.2002.
4. **Gempp E**, **Louge P.** Inner ear decompression sickness in scuba divers: a review of 115 cases. *Eur Arch Otorhinolaryngol* 270: 1831–1837, 2013. doi:10.1007/s00405-012-2233-y.
5. **Mitchell SJ**, **Doolette DJ.** Selective vulnerability of the inner ear to decompression sickness in divers with right to left shunt: the role of tissue gas supersaturation. *J Appl Physiol (1985)* 106: 298–301, 2009. doi:10.1152/japplphysiol.90915.2008.
6. **Imbert JP**, **Bontoux M.** Diving data bank: a unique tool for diving procedures development. *20th Annual Offshore Technology Conference*. Houston, TX: Offshore Technology Conference, 1988.
7. **Gardette B.** Correlation between decompression sickness and circulating bubbles in 232 divers. *Undersea Biomed Res* 6: 99–107, 1979.
8. **Thalmann ED.** Testing of revised unlimited-duration upward excursions during helium-oxygen saturation dives. *Undersea Biomed Res* 16: 195–218, 1989.
9. **Spaur WH**, **Thalmann ED**, **Flynn ET**, **Zumrick JL**, **Reedy TW**, **Ringelberg JM.** Development of unlimited duration excursion tables and procedures for helium-oxygen saturation diving. *Undersea Biomed Res* 5: 159–177, 1978.
10. **Barnard EEP.** Fundamental studies in decompression from steady-state exposures. In: *Underwater Physiology V*, edited by Lambertsen CJ. Bethesda, MD: FASEB, 1976, p. 263–271.
11. **Leitch DR.** Medical aspects of a simulated dive to 1,500 feet (458 metres). *Proc R Soc Med* 64: 1273–1276, 1971.
12. **Brubakk AO**, **Peterson R**, **Grip A**, **Holand B**, **Onarheim J**, **Segadal K**, **Kunkle TD**, **Tonjum S.** Gas bubbles in the circulation of divers after ascending excursions from 300 to 250 msw. *J Appl Physiol (1985)* 60: 45–51, 1986. doi:10.1152/jappl.1986.60.1.45.
13. **Lambertsen CJ**, **Gelfand R**, **Clark JM.** *Predicitive studies IV. Work capability and physiological effects in He-O2 excursions to pressures of 400, 800, 1200, and 1600 feet of sea water (Technical Report)*. Philadelphia, PA: University of Pennsylvania, Institute of Environmental Medicine, 1978.
14. **Spaur WH.** U.S. Navy operational experience. In: *Development of Decompression Procedures for Depths in Excess of 400 Feet*, edited by Hamilton RW. Bethesda, MD: Undersea Medical Society, 1976, p. 181–184.
15. **Buhlmann AA**, **Gehring H.** Inner ear disorders resulting from inadequate decompression—"vertigo bends". In: *Underwater Physiology V*, edited by Lambertsen CJ. New York: Academic Press, 1976, p. 341–347; discussion p. 373–348.
16. **Spencer MP.** Decompression limits for compressed air determined by ultrasonically detected blood bubbles. *J Appl Physiol* 40: 229–235, 1976. doi:10.1152/jappl.1976.40.2.229.
17. **Eatock BC**, **Nishi RY.** Doppler ultrasonic detection of intravascular bubbles during decompression from the 1985 CAN/UK saturation dives to 100 and 360 msw (Technical Report). Downsview (ON, CAN): Defence and Civil Institute of Environmental Medicine, 1986.
18. **Doolette DJ**, **Upton RN**, **Grant C.** Altering blood flow does not reveal difference between nitrogen and helium kinetics in brain or in skeletal muscle in sheep. *J Appl Physiol (1985)* 118: 586–594, 2015. doi:10.1152/japplphysiol.00944.2014.
19. **Srinivasan RS**, **Gerth WA**, **Powell MR.** Mathematical models of diffusion-limited gas bubble dynamics in tissue. *J Appl Physiol (1985)* 86: 732–741, 1999. doi:10.1152/jappl.1999.86.2.732.
20. **Srinivasan RS**, **Gerth WA.** *Mathematical models of diffusion-limited gas bubble evolution in perfused tissue (Technical Report)*. Panama City, FL: Navy Experimental Diving Unit, 2013.
21. **Gutvik CR**, **Dunford RG**, **Dujic Z**, **Brubakk AO.** Parameter estimation of the Copernicus decompression model with venous gas emboli in human divers. *Med Biol Eng Comput* 48: 625–636, 2010. doi:10.1007/s11517-010-0601-6.
22. **Solano-Altamirano JM**, **Goldman S.** The lifetimes of small arterial gas emboli, and their possible connection to Inner Ear Decompression Sickness. *Math Biosci* 252: 27–35, 2014. doi:10.1016/j.mbs.2014.03.008.
23. **Tikuisis P**, **Ward CA**, **Venter RD.** Bubble evolution in a stirred volume of liquid closed to mass transport. *J Appl Phys* 54: 1–9, 1983. doi:10.1063/1.331741.
24. **Hrncir E**, **Rosin J.** Surface tension of blood. *Physiol Res* 46: 319–321, 1997.
25. **Lango T**, **Morland T**, **Brubakk AO.** Diffusion coefficients and solubility coefficients for gases in biological fluids: a review. *Undersea Hyperb Med* 23: 247–272, 1996.
26. **Hills BA**, **Butler BD.** Size distribution of intravascular air emboli produced by decompression. *Undersea Biomed Res* 8: 163–170, 1981.
27. **Butler BD**, **Hills BA.** The lung as a filter for microbubbles. *J Appl Physiol Respir Environ Exerc Physiol* 47: 537–543, 1979. doi:10.1152/jappl.1979.47.3.537.
28. **Landolt JP**, **Money KE**, **Topliff ED**, **Nicholas AD**, **Laufer J**, **Johnson WH.** Pathophysiology of inner ear dysfunction in the squirrel monkey in rapid decompression. *J Appl Physiol Respir Environ Exerc Physiol* 49: 1070–1082, 1980. doi:10.1152/jappl.1980.49.6.1070.
29. **Verstappen FT**, **Bernards JA**, **Kreuzer F.** Effects of pulmonary gas embolism on circulation and respiration in the dog. III. Excretion of venous gas bubbles by the lung. *Pflugers Arch* 370: 67–70, 1977. doi:10.1007/BF00707947.
30. **Sastry S**, **Daly K**, **Chengodu T**, **McCollum C.** Is transcranial Doppler for the detection of venous-to-arterial circulation shunts reproducible? *Cerebrovasc Dis* 23: 424–429, 2007. doi:10.1159/000101466.
31. **Barak OF**, **Madden D**, **Lovering AT**, **Lambrechts K**, **Ljubkovic M**, **Dujic Z.** Very few exercise-induced arterialized gas bubbles reach the cerebral vasculature. *Med Sci Sports Exerc* 47: 1798–1805, 2015. doi:10.1249/MSS.0000000000000625.
32. **Eldridge MW**, **Dempsey JA**, **Haverkamp HC**, **Lovering AT**, **Hokanson JS.** Exercise-induced intrapulmonary arteriovenous shunting in healthy humans. *J Appl Physiol (1985)* 97: 797–805, 2004. doi:10.1152/japplphysiol.00137.2004.
33. **Zavorsky GS**, **Walley KR**, **Russell JA.** Red cell pulmonary transit times through the healthy human lung. *Exp Physiol* 88: 191–200, 2003. doi:10.1113/eph8802418.
34. **Westerhof N**, **Bosman F**, **De Vries CJ**, **Noordergraaf A.** Analog studies of the human systemic arterial tree. *J Biomech* 2: 121–143, 1969. doi:10.1016/0021-9290(69)90024-4.
35. **Bogren HG**, **Buonocore MH.** Blood flow measurements in the aorta and major arteries with MR velocity mapping. *J Magn Reson Imaging* 4: 119–130, 1994. doi:10.1002/jmri.1880040204.
36. **Robson PM**, **Dai W**, **Shankaranarayanan A**, **Rofsky NM**, **Alsop DC.** Time-resolved vessel-selective digital subtraction MR angiography of the cerebral vasculature with arterial spin labeling. *Radiology* 257: 507–515, 2010. doi:10.1148/radiol.092333.
37. **Flook V.** Excusion tables in saturation diving—decompression implication of current UK practice (Research Report). Norwich, UK: *Health and Safety Executive (UK)*, 2004.
38. Report from the Petroleum Safety Authority diving database DSYS—2021. Stavanger, Norway: Petroleumstilsynet, 2021.